Transaction B: Mechanical Engineering
Vol. 17, No. 2, pp. 102–107

SCIENTIA IRANICA

On the Relationship Between Unsteady Forces and Shock Angles on a Pitching Airplane Model

A.R. Davari[1,*] and M.R. Soltani[2]

Abstract. *A series of supersonic visualization tests were performed on an airplane model in both static and dynamic pitching cases. After image processing, the wave angles originating from different parts of the model were carefully measured and averaged over several oscillation cycles. These findings were then compared with the corresponding normal force under similar conditions. The results reveal a hysteresis loop in variations of the model shock angles with instantaneous angles of attack during up-stroke and down-stroke motions. In comparison with the normal force hysteresis loop, it has been found that there is an interesting relationship between the shape of the hysteresis loop of the shock angle and the corresponding loop observed in the normal force data. Further, the oscillation frequency has been shown to have similar effects on both shock angle and aerodynamic force variations with the instantaneous angle of attack.*

Keywords: *Hysteresis; Pitching motion; Vortex bursting; Reduced frequency; Schlieren; Up-stroke.*

INTRODUCTION

Aggressive maneuvering in aircraft and missiles can cause overshoots in angles of attack well beyond static stall conditions. In time dependent motion, the lateral and longitudinal positions of various vortices formed over the aircraft parts, i.e. wings, forebody, etc., change as a function of the angle of attack which itself is a function of time. The introduction of time into an already rather complex flow makes the transient flow particularly difficult. Rapid changes of incidence produce a large phase lag between the angle of attack and the flow field.

In an oscillatory motion, there exists a different flow structure over the wing during the up and down stroke motions, forming a hysteresis loop in the corresponding aerodynamic behavior. As a result of this hysteresis in the flow structure, in an oscillatory motion, the values of the aerodynamic forces and moments differ between up and down stroke motions.

A large overshoot in maximum forces and moments and a delay in the stall angle of attack, compared to the static data, are characteristics of the flowfield during upward motion. However, in downward motion, the dynamic values are substantially less than the corresponding static ones. Thus, in an oscillatory motion, variations of the aerodynamic forces and moments with time have a phase lag compared to the corresponding harmonic variations of the instantaneous angle of attack. This phase lag is due to the time lag in the flow structure. The magnitude of the overshoots and the size of the hysteresis loops are strong functions of the reduced frequency.

Numerous investigations were carried out on the characteristics of the hysteresis loops and their mechanisms. These investigations have been mainly focused on the effects of oscillation frequency and amplitude on the hysteresis loops of the aerodynamic forces and moments [1,2]. Even though valuable information has been obtained on the relationship between oscillation parameters and corresponding aerodynamic characteristics, to the author's knowledge, no attempt has been made to relate the shape and attitude of the unsteady shock waves on an oscillating body to its aerodynamic behavior.

In this paper, the shock angles emanating from different parts of an airplane model in a pitching motion were measured. The results were compared with the normal force measured on this model. The comparisons show that variations of the shock angle

1. *Department of Mechanical and Aerospace Engineering, Islamic Azad University, Science and Research Campus, Poonak, Tehran, P.O. Box 14155-4933, Iran.*
2. *Department of Aerospace Engineering, Sharif University of Technology, Tehran, P.O. Box 11155-9567, Iran.*
*. *Corresponding author. E-mail: ardavari@srbiau.ac.ir*

Received 16 May 2009; received in revised form 14 November 2009; accepted 9 January 2010

with the instantaneous angle of attack are similar to those of the normal force.

EXPERIMENTAL SETUP AND DATA PROCESSING

The experiments were conducted in a 60 cm×60 cm tri-sonic continuous wind tunnel with a Mach number ranging from 0.4 to 4.0. The model considered in the present experiments was the well known standard dynamics model, SDM [3-6]. SDM is a generic fighter airplane with wing leading edge extensions, ventral fins and air intake. The model manufactured for the present experiments was made of steel and had a length to maximum diameter ratio of about 7.0. This model was tested at a constant Mach number of 1.5. A mechanism consisting of rods and arms was used to convert the rotating motion of an electric motor into a reciprocating motion and transfer it to the model. The oscillation frequency of the model was controlled by setting the electric motor rpm. A five component dynamic strain gauge balance was used to measure the aerodynamic forces and moments [6]. The balance calibration procedure consisted of applying loads in different directions and measuring the output signal. The interference effects have also been taken into account. A calibration rig was manufactured for this purpose. Force measurement experiments were conducted in both wind-off and wind-on cases and the tares were then subtracted from the wind-on data.

The unsteady supersonic waves have been visualized using the Schlieren system during a pitching oscillation at different frequencies and mean angles of attack, as shown in Figure 1b.

The instantaneous angle of attack was measured using a potentiometer attached to the oscillation system. Some processing was undertaken on the basic Schlieren images to have a clear view of the shock waves and to facilitate the shock angle measurements on the images. For this purpose, the background color was first subtracted from the original image (Figure 1c) and then the contrast of the resulting image was increased, as shown in Figure 1d. These processes were performed on the RGB information of each pixel in the original image [7].

Figure 2 shows the parameters measured on the processed images. The measurements were carried out for several oscillation cycles and the data have been then averaged over the up-stroke and down-stroke cycles individually.

The average of the absolute deviations of the data points from their means, in the static and dynamic cases, was chosen to be a characteristic for data uncertainty. Figure 3 shows the error bars indicating the uncertainties for both static and dynamic data.

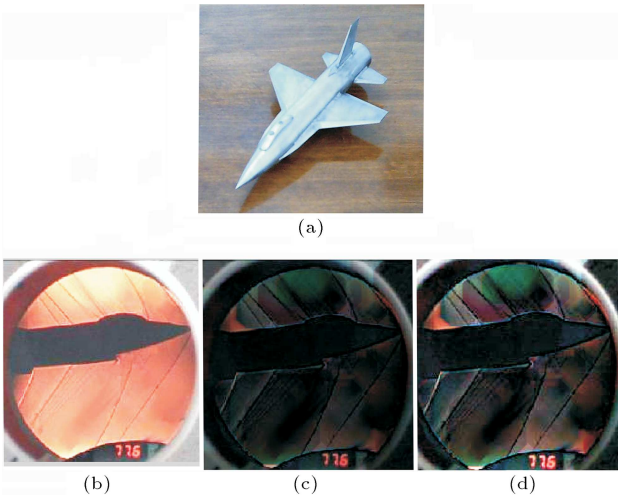

Figure 1. The model and the image processing steps.

DISCUSSION

The experiments were performed under both static and dynamic pitching conditions at a constant Mach number of 1.5 for two different reduced frequencies. The static results followed by the dynamic ones, are presented in the following sections.

Static Condition

Figure 4 shows variations of the shock angles originating from the canopy and the wing leading edge at the upper surface, as a function of the static angle of attack, with the right vertical axis showing the static $C_{N\alpha}$. For the canopy, the shock angle starts to increase near $\alpha = 4°$. A smaller second increase is also seen, starting around $\alpha = 7°$.

On the other hand, the wing shock angle first

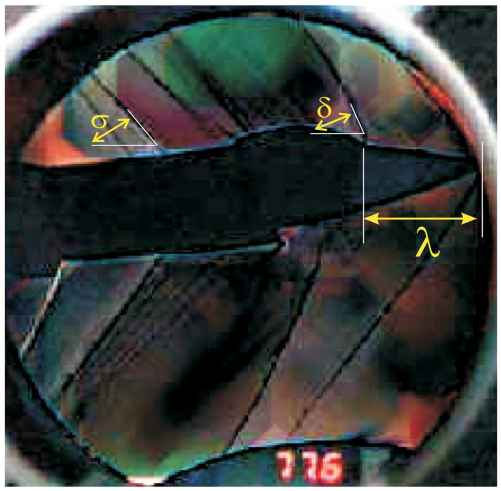

Figure 2. The parameters measured on the processed image.

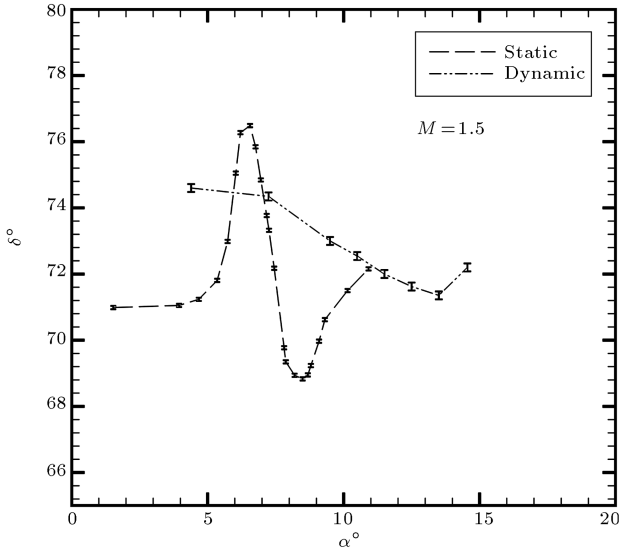

Figure 3. Typical measurement uncertainties for both static and dynamic cases.

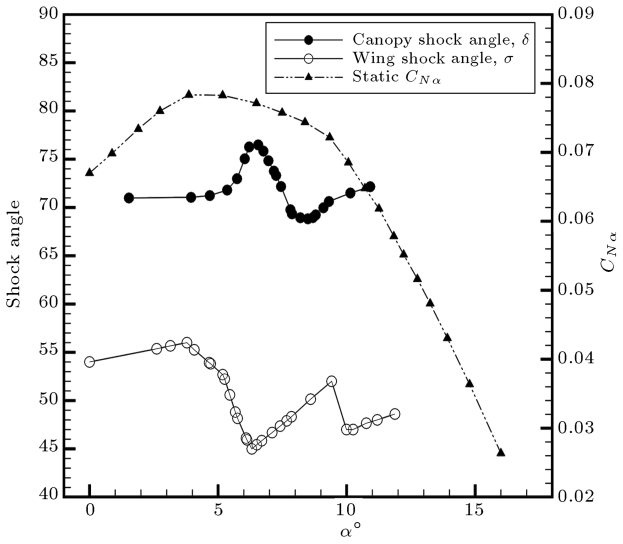

Figure 4. Variations of the static shock angles with angle of attack, $M_\infty = 1.5$.

decreases at $\alpha = 4°$, then, starts to increase at about $\alpha = 7°$ and decreases again near $\alpha = 9°$.

Note that the wing sweep angle is about 45 and the LEX sweep angle is 70 degrees. The force measurements on the model [6] revealed that the potential flow separation occurs at around a 5 degree angle of attack, while the leading edge vortex on the LEX starts to form near $\alpha = 10°$ [8]. It seems that the flow separation on the wing and the vortical flow formation on the LEX are major contributors to the sudden changes in the shock angle on the wing leading edge, as seen in Figure 4. However, these two factors also affect the canopy shock attitude through the boundary layer. For this reason, the increases and decreases seen in Figure 4, for both the canopy and the wing, nearly occur at the same angles of attack.

Considering the variations of the slope of the normal force with angle of attack, $C_{N\alpha}$, as a function of the static angle of attack, a noticeable decrease near $\alpha = 4°$ is observed and a gentle second decrease is also seen near $\alpha = 9°$.

Thus, decreasing the wing shock angle is accompanied by a corresponding decrease in the slope of the normal force, indicating a slow rate of increase of C_N with the angle of attack. In this way, the wing shock angle can be related to the static normal force. At a constant free stream Mach number, as wing shock angle, σ, decreases, the shock gets closer to the wing surface. The flow separation on the wing and the vortical flow of LEX gives rise to the static pressure on the wing upper surface, as stated earlier. This leads to a lower rate of increasing the normal force with the angle of attack. Note that for a constant Mach number of 1.5, as the angle of attack increases, the wing shock angle will also be increased. However, it seems that the flow separation over the wing upper surface, starting near $\alpha = 4°$ [6], has been convected upstream to the leading edge shock through the boundary layer and has decreased the shock-wing clearance. Also, near $\alpha = 10°$, the strake vortex starts to form [9]. Effects of this vortex propagating downstream on the wing shock have also decreased the wing shock angle for the second time while the canopy shock remains unaffected by this vortex.

Oscillatory Pitching Motion

Figure 5 shows the variations of the canopy shock angle with instantaneous angle of attack for two mean angles of 3 and 8 degrees at a constant reduced frequency of $k = 0.003$. The variation of the dynamic normal force coefficient, C_N, is also shown on the right axis for comparison.

A hysteresis loop is observed in variations of the dynamic C_N with the instantaneous angle of attack, which is an indication of the lead and lag effects between the instantaneous flow field and the model motion [6]. A cross over point in the hysteresis loop of C_N is seen near the mean value of the angle of attack in both Figures 5a and 5b, forming a *figure-8* shape. This phenomenon is due to a switch between the lead and the lag of the flow field and the instantaneous angle of attack [9].

It is interesting to note that a hysteresis loop is also observed in variations of the canopy shock angle with the instantaneous angle of attack. The same behavior can be seen in Figure 6 for variations of the wing leading edge shock angle where the difference in the up-stroke and down-stroke shock angles resembles a hysteresis loop.

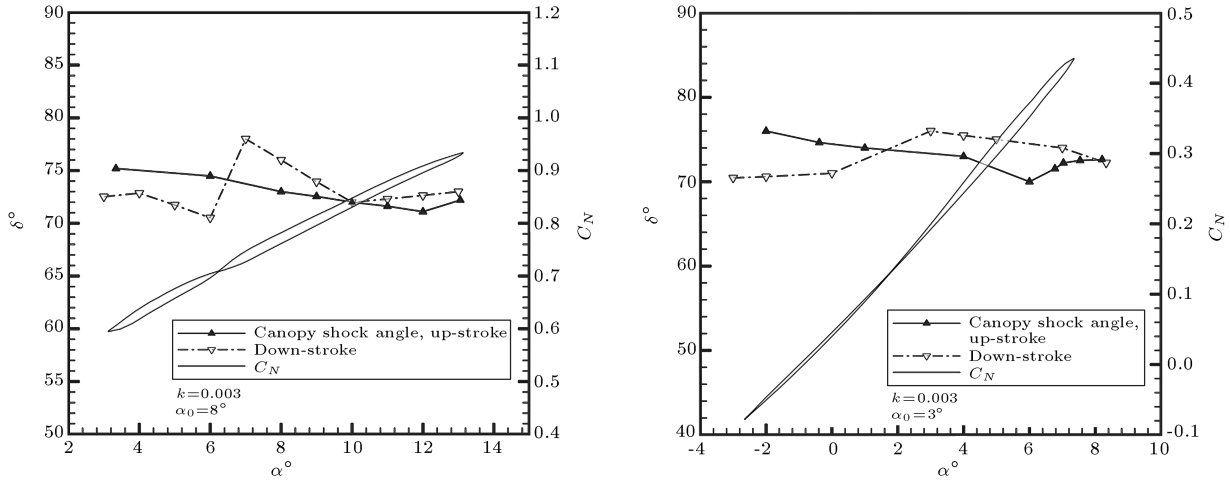

Figure 5. Variations of the canopy shock angle in pitching motion, $M_\infty = 1.5$.

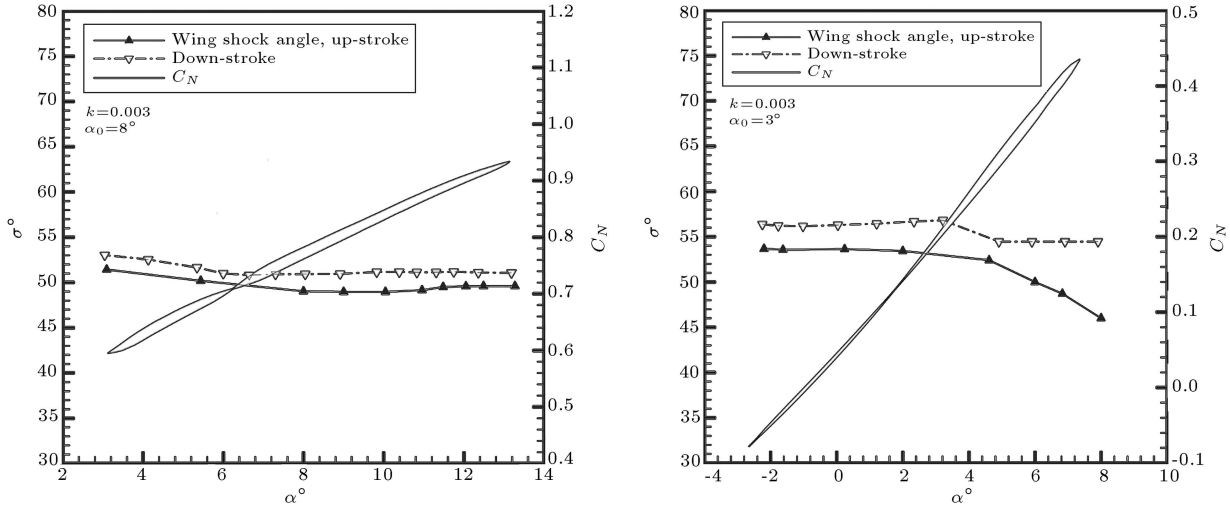

Figure 6. Variations of the wing leading edge shock angle in pitching motion, $M_\infty = 1.5$.

The most important phenomenon observed in Figure 5 is the coincidence of the cross-over angle of attack for both the canopy shock and normal force hysteresis loops, i.e. the angle of attack at which the hysteresis loops form a *figure-8* shape is the same for both the normal force and the canopy shock angle. The wing shock angle variations with the angle of attack also exhibit a hysteresis loop, but the variations, as seen from Figure 5, do not form the *figure-8* shape.

As seen earlier, the hysteresis behavior of the canopy shock angle is similar to the normal force loop. This implies that during an oscillatory pitching motion, among the shocks originating from different parts of the model, the canopy shock may be considered as being dominant and the aerodynamic behavior during pitching oscillations depends on the strength and inclination angle of this shock; the wing shock angle does not seem to have a strong effect on the shape and characteristics of the normal force hysteresis loop.

Figures 7 and 8 show the effects of reduced frequency on both the canopy shock angle and the canopy shock stand-off distance measured from the nose apex. As observed earlier, the impact of the canopy shock on the unsteady aerodynamic behavior of the model is more pronounced than that originating from the wing leading edge at the upper surface.

According to Figure 7, the canopy wave angle increases as the reduced frequency is increased. For $k = 0.001$, this angle is slightly more than in the static case. However, for $k = 0.003$, the increase in the shock angle is more evident. This increase in the shock angle, as illustrated in Figure 2, means that the curved segment of the bow shock ahead of the canopy tends to combine with the normal segment, forming a stronger shock. The increased shock strength promotes the consequences of shock induced separation on the lee side and, as a result, the normal force decreases as the reduced frequency increases.

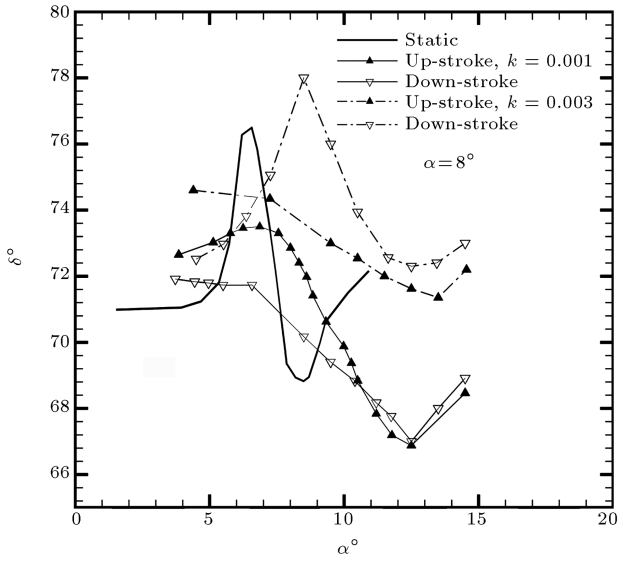

Figure 7. Effects of the reduced frequency on canopy shock angle variations, $M_\infty = 1.5$.

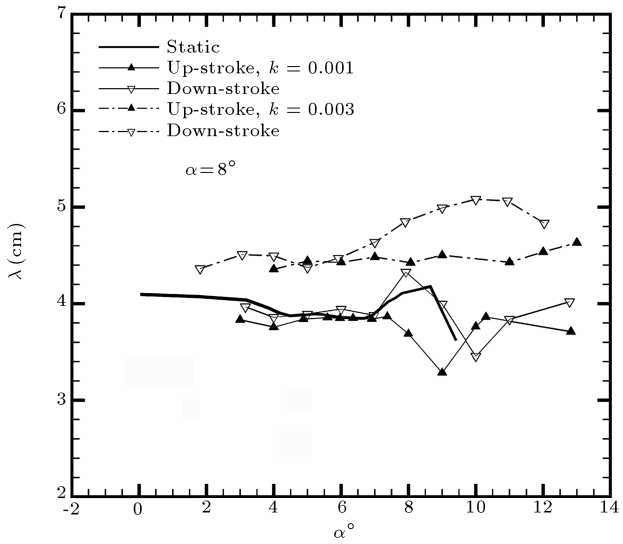

Figure 8. Effects of the reduced frequency on canopy shock stand off distance, $M_\infty = 1.5$.

Further, a cross-over is observed in the hysteresis loop of the canopy shock angle for $k = 0.003$, causing the hysteresis loop of the normal force to form a *figure-8* shape at this reduced frequency. Also, note that for both static and dynamic cases, a jump can be observed in the canopy shock angle variations with α. The angle of attack at which this jump occurs increases as the reduced frequency increases from $k = 0.0$ (static case) to $k = 0.003$. The observed jump in the canopy shock angle is probably due to the potential flow separation from the ogival nose of the model. According to Figure 6, as the reduced frequency increases, the flow separation is delayed until higher angles of attack. This may be an indication of the moving wall effect [10].

A similar trend is observed in the shock stand-off distance shown in Figure 8. As the reduced frequency increases from zero to $k = 0.003$, the stand-off distance also increases. According to Figure 2, the shock moves downstream towards the canopy base, as λ increases, indicating that the bow shock tends to attach to the canopy forming a stronger shock. In this situation, the lee side pressure increases and the normal force decreases. This represents another aspect of reduced frequency effects on the normal force, which is shown to be related to the canopy shock angle and its stand-off distance. As the reduced frequency increases, the canopy bow shock tends to attach to the canopy base and its curved part is straightened, approaching a normal shock. The overall consequence is an increase in the lee side shock strength and decrease in the total normal force.

The balance force data on this model shown in Figure 9 confirm that the normal force on the model decreases as the reduced frequency increases. Note that for the highest reduced frequency examined here, $k = 0.005$, the flow field can no longer follow the fast angle of attack changes and, consequently, the normal force remains nearly constant during the whole oscillation cycle.

Further, according to Figure 8, note that for both reduced frequencies during the up-stroke motion, the canopy shock moves away from the canopy base; during the down stroke it gets closer to the canopy forming a hysteresis loop. This implies that normal force during the up-stroke is higher than that of the down-stroke motion, which is in agreement with directions shown in Figure 9.

Also, it can be observed that the angle of attack and the reduced frequency for the occurrence of cross-

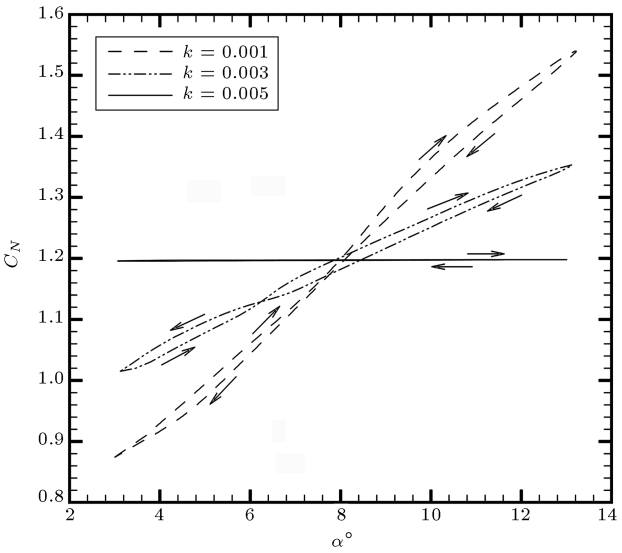

Figure 9. Effects of the reduced frequency on the model normal force, $M_\infty = 1.5$.

over in the normal force hysteresis loop in Figure 9 are nearly the same as those in which the canopy shock angle forms *figure-8*, i.e. $\alpha \approx 6.5^\circ$ and $k = 0.003$.

It is important to note that the conical shock at the nose apex, though seemingly to be effective on unsteady aerodynamic behavior, has not been considered in the present experiments due to some limitations on the model and the schlieren window size. Thus, the model nose shock angle behavior can be considered a missing feature of the present work.

However, in this paper, the canopy and the wing leading edge shock angles are compared to normal force behavior in both static and dynamic cases. The physical phenomena observed in variations of the normal force were, then, related to the wing and canopy shock attitudes.

CONCLUSION

The shock wave attitude emanating from different parts of an airplane model during pitching motion were studied, using the schlieren photographs. The results revealed a hysteresis loop in variations of the shock angle with the instantaneous angle of attack during upstroke and down stroke motions. It has been found that there is a direct correspondence between the attitude of the shock waves originating from the canopy, wing, etc, and the model aerodynamic behavior. The static aerodynamic characteristics are very similar to the behavior of the wing leading edge shock status. In turn, in dynamic cases, the hysteresis loops for the canopy shock angle variations is closely related to the hysteresis loop of the normal force. It has been deduced that the aerodynamic characteristics of the model are determined by the wing shock angle in the static case and in an oscillatory pitching motion the canopy and, probably, the nose shock angles are the dominant ones.

NOMENCLATURE

α	instantaneous angle of attack
$\alpha_\circ$	mean angle of attack
f	oscillation frequency, Hz
c	the wing mean aerodynamic chord, m
$k = 2\pi fc/V_8$	reduced frequency
C_N	model normal force coefficient
$C_{N\alpha}$	slope of the static normal force with angle of attack,/deg.
σ	wing leading edge shock angle
δ	canopy shock angle
λ	canopy shock stand off distance measured from the nose apex, cm

REFERENCES

1. Sunada, S., Kawachi, K., Matsumoto, A. and Sakaguchi, A. "Unsteady forces on a two-dimensional wing in plunging and pitching motions", *AIAA Journal*, **39**(7), pp. 1230-1239 (2001).
2. Brunton, S. et al. "Unsteady aerodynamic forces on small-scale wings: Experiments, simulations and models", *AIAA 2008-520* (2008).
3. Beyers, M.E. "SDM pitch and yaw axis stability derivatives", *AIAA 85-1827* (1985).
4. Schmidt, E. "Standard dynamics model experiments with the DFVLR/AVA transonic derivative balance", *AGARD CP-386* (1985).
5. Jansson, T. and Torngren, L. "New dynamic testing techniques and related results at FFA", *AGARD CP-386* (1985).
6. Soltani, M.R. and Davari, A.R. "Identification of a new similarity parameter to investigate the unsteady aerodynamic behavior of an aircraft in pitching motion", *The Aeronautical Journal*, **108**(1086), pp. 427-434 (2004).
7. Gonzalez, R.C. and Woods, R.E., *Digital Image Processing*, 2nd Ed., Prentice Hall, pp. 282-344 (2002).
8. Soltani, M.R., Bragg, M.B. and Brandon, J.M. "Measurements on an oscillating 70 degree delta wing in subsonic flow", *Journal of Aircraft*, **27**(3), pp. 211-217 (1990).
9. Wentz, W.H. "Wind tunnel investigations of vortex break downs", PhD Dissertation, University of Kansas, Lawrence, KS (1968).
10. Ericsson, L.E. and Beyers, M.E. "Universality of the moving wall effect", *Journal of Aircraft*, **37**(3), pp. 508-513 (2000).

BIOGRAPHIES

Mohammad Reza Soltani, a professor in the aerospace engineering department of Sharif University of Technology, Tehran, has a PhD in aerodynamics from the University of Illinois at Urbana-Champaign, USA. His research interests include applied aerodynamics, unsteady aerodynamics wind tunnel testing, wind tunnel design, and data processing.

Ali Reza Davari is assistant professor in the department of mechanical and aerospace engineering at the science and research campus of the Islamic Azad University in Iran. He has conducted several experimental studies on unsteady aerodynamics and interference effects. He is also interested in new prediction and optimization methods in aerodynamics, such as neural networks and evolutionary algorithms. He graduated with a PhD degree in 2006 and has published over 11 journal papers since that time.